Treatment of Breast and Colon Cancer Cell Lines with Anti-Helmintic Benzimidazoles Mebendazole or Albendazole Results in Selective Apoptotic Cell Death

Jakeb SSM Petersen
University of Otago - Dunedin Campus: University of Otago
Sarah Baird (s.baird@otago.ac.nz)
University of Otago - Dunedin Campus: University of Otago https://orcid.org/0000-0001-6741-5866

Research Article

Keywords: tubulin, cell cycle, anti-helmintic, repurposing, apoptosis

Posted Date: April 30th, 2021

DOI: https://doi.org/10.21203/rs.3.rs-450663/v1

Abstract

Purpose: Anti-helmintic drugs mebendazole and albendazole are commonly used to treat a variety of parasitic infestations. They have recently shown some promising results in pre-clinical in vitro and in vivo anti-cancer studies. We compare their efficacy in breast and colon cancer cell lines as well as in non-cancerous cells and elucidate their mechanism of action.

Methods: The drugs were screened for cytotoxicity in MDA-MB-231, MCF-7 (breast cancer), HT-29 (colorectal cancer) and mesenchymal stem cells, using the MTT assay. Their effects on the cell cycle, tubulin levels and cell death mechanisms were analysed using flow cytometry and fluorescent microscopy.

Results: Mebendazole and albendazole were found to selectively kill cancer cells, being most potent in the colorectal cancer cell line HT-29, with both drugs having IC50 values of less than 1 μM at 48 hours. Both mebendazole and albendazole induced classical apoptosis characterised by caspase-3 activation, phosphatidylserine exposure, DNA fragmentation, mitochondrial membrane permeability and reactive oxygen species production. Cell cycle arrest in the G2/M phase was found, and tubulin polymerisation was disrupted.

Conclusion: Mebendazole and albendazole cause selective cancer cell death via a mechanism of classical apoptosis and cell cycle arrest, which involves the destabilisation of microtubules.

Introduction

Mebendazole (MBZ) and albendazole (ABZ) are broad-spectrum benzimidazole anti-helmintic drugs. They are commonly prescribed to treat a range of parasitic worm infections in humans and domestic animals. These drugs have few adverse effects and low cost [1]. The anti-helmintics bind to the colchicine-binding domain of tubulin and inhibit microtubule polymerisation, leading to reduced glucose uptake in the gastrointestinal cells of helminths [2].

MBZ and ABZ have recently been shown to have promising anti-cancer effects in a range of *in vitro* studies [3-11], as well as in a small number of xenograft models [9,12]. MBZ has also been shown to act in synergy with ionising radiation in melanoma and small cell lung cancer [13] and with non-steroidal anti-inflammatory sulindac in colorectal cancer [12].

Here, we compare this information with the cytotoxicity of MBZ and ABZ in breast and colorectal cancer cell lines and in non-cancerous mesenchymal stromal cells, and describe the mechanism of action by measuring cell cycle progression, microtubule changes and markers of apoptosis, necrosis and oxidative stress.

Materials And Methods

Materials

Dimethyl sulfoxide (DMSO) was purchased from Scharlau (Barcelona, Spain). Fetal bovine serum (FBS), penicillin-streptomycin, PBS and trypsin were from Gibco (Carlsbad, CA). 3-(4,5-dimethylthiazol-2-yl)-2,5-diphenyl tetrazolium bromide (MTT), mebendazole and albendazole were purchased from Sigma-Aldrich (St. Louis, MO). Paclitaxel was purchased from Cayman Chemical (Michigan, USA). Anti-α-tubulin (DM1A) mouse antibody and anti-acetyl-α-tubulin (Lys40) (D20G3) rabbit antibody were from Cell Signaling Technology (MA, USA).

Cell Culture

The three human cancer cell lines were MCF-7 (breast adenocarcinoma), MDA-MB-231 (triple negative breast cancer, kind gifts from Prof. Rhonda Rosengren) and HT-29 (colorectal adenocarcinoma, ATCC). The non-cancerous, human bone marrow-derived mesenchymal stromal cell (MSC) line RCB2157 (Riken Biosciences) was also used. All cell lines were cultured in Dulbecco's Modified Eagle Medium (DMEM) with 5% heat inactivated FBS for cancer cell lines and 10% for MSCs, 100 units/mL penicillin and 100 µg/mL streptomycin. Cells were incubated at 37^{o}C in humidified conditions with 5% CO_2.

MTT Assay

Cells were seeded and allowed to adhere overnight. They were then treated with MBZ, ALB or DMSO as a vehicle control at 0.1% v/v. The quantity of live cells remaining following 24 and 48hr treatment exposure was measured using the MTT assay, which assesses mitochondrial and endoplasmic reticulum dehydrogenase activity [14]. MTT was added to cells at a final concentration of 0.5 mg/mL, and incubated at 37^{o}C for 3 hrs. Formazan crystals were dissolved with DMSO, and the resulting absorbance read at 560 nm using the spectrophotometer.

Flow Cytometry

Flow cytometry was carried out using a BD FACSCantoII® flow cytometer and data analysed using FlowJo® VX software. Cells were treated and after either 24 or 48 hrs were prepared and stained as outlined below, then analysed using the appropriate filters of FITC and/or PE.

Phosphatidylserine exposure

Following incubation with treatments for 24 or 48 hrs, cells and media were harvested, centrifuged at 4^{o}C, 2000 rpm for 3 mins, the pellet washed twice in 4^{o}C PBS and the cells resuspended in Annexin V binding buffer (HEPES; 10.0 mM (pH 7.4), NaCl; 140.0 mM, and CaCl2; 2.5 mM) with propidium iodide (PI) and Annexin V conjugated to FITC. Cells were incubated for 15 min in the dark at room temperature.

Mitochondrial membrane permeability

Cells were treated and harvested, the pellet washed twice in 4^{o}C PBS and the cells resuspended in PBS. Tetramethylrhodamine ethyl ester (TMRE) was added to a final concentration of 40 nM, then incubated at 37^{o}C for 10 mins.

Cell Cycle

Following incubation with treatments for 24 or 48 hrs, media and cells were harvested, centrifuged at 4^{o}C, 2000 rpm for 3 mins, washed twice in 4^{o}C PBS and fixed with 70% ethanol at 4^{o}C for 30 mins. Cell were washed twice in phosphate-citrate buffer (Na_2HPO_4; 192 mM, citric acid; 4 mM (pH 7.8)), treated with 100 µg/mL RNAse A and stained with 50 µg/mL PI.

Caspase activation

Following treatment of cells for 24 or 48 hours, media and cells were harvested, washed in cold PBS and frozen at -80^{o}C overnight. Cells were then resuspended in buffer (100mM HEPES, 10% sucrose, 0.1% CHAPS, 10^{-4}% Tergitol NP-40 at pH 7.25), DTT added to 5 mM and Ac-DEVD-AMC caspase substrate added to 50 µM. The plate was incubated in the dark for 2 hours and the AMC fluorescence read at excitation 360nm and emission 460nm.

Oxidative stress

Oxidative stress levels were analysed by measuring reduced thiol content using the DTNB (5, 5”-dithio-bis-(2-nitrobenzoic acid)) assay. DTNB quantifies free sulfhydryl groups by producing a measurable yellow product [15]. Using the molar extinction coefficient of 14,150 M^{-1} cm^{-1} the free sulfhydryl content can be calculated. Cells were treated, incubated at 37^{o}C for 48 hrs, harvested and centrifuged at 4^{o}C, 2000 rpm for 3 mins, washed with PBS twice and sonicated for 2 mins. Ten % SDS and DTNB at final concentration 30 µM were added and incubated at room temperature for 30 mins. Absorbance was measured at 412 nm.

Fluorescent Microscopy

For staining with anti-tubulin antibodies, cells were treated with for 8 hours. Following fixation, cells were blocked for 60 mins in blocking buffer (1X PBS, 5% BSA, 0.3% Triton X-100) and stained with primary antibody, anti-α-tubulin at 1:16,000 or anti-acetyl-α-tubulin at 1:800, overnight at 4^{o}C. After washing, cells were incubated with secondary antibodies and Hoechst 33342 at 10 µg/mL for 1 hour at room temperature in the dark. Prolong Gold was placed on the slides along with coverslips. The cells were analysed using the Nikon AI-R inverted fluorescent microscope with Nikon Intensilight C-HGFI mercury lamp (Olympus, Japan) at 20x magnification.

Statistical Analyses

Results were analysed using GraphPad Prism® 6.0 software. Cell viability, flow cytometry and DTNB experiments (N=3) were analysed using one-way analysis of variance (ANOVA) and Dunnett's post hoc tests with statistical significance at P<0.05.

Results

MBZ and ABZ lower cancer cell viability, especially in colorectal cancer cell line HT29

The IC_{50} values of MBZ and ABZ over 48 hours were determined in three cancer cell lines MCF-7, MDA-MB-231 (both breast cancer) and HT-29 (colon cancer), as well as in the non-transformed mesenchymal stromal-cell line RCB2157, using MTT cell viability assays (Fig 1a-d). The IC_{50} values in the mesenchymal stromal cell line RCB2157 were the highest by several fold (Table 1). The two breast cancer lines were less sensitive to the two drugs than the colorectal cancer cell line HT29.

MBZ and ABZ block the cell cycle at G2/M

Further analyses were carried out in the HT29 cells to determine the mechanism of the loss of cell viability after 24 or 48 hours treatment with MBZ or ABZ. Progression through the cell cycle was analysed using fixation and staining with propidium iodide (PI). Paclitaxel, known to cause a block in the cell cycle at G2/M through binding to microtubules, was used as a positive control.

Treatment with 2 μM MBZ or ABZ or 50 nM paclitaxel resulted in significantly large increases in the G2/M phase compared to control (Fig. 1e-f). At 24 hours, MBZ was at 60.18%, ABZ at 58.68% and paclitaxel at 62.42% compared to vehicle-only control at 21.37% (P > 0.05). There were smaller, but still significant increases of cells in the >G2/M phase, and concomitant decreases in the proportion of cells in the G1 and S phases.

MBZ and ABZ induce apoptotic nuclear morphology and depolymerise microtubules

In order to investigate whether MBZ and ABZ interact with microtubules in a similar way to paclitaxel, HT-29 cells were stained for nucleus and microtubules following treatment with MBZ (2 μM), ABZ (2 μM), paclitaxel (50 nM) or DMSO vehicle control (0.1% v/v) for 8 hrs. Hoechst 33342 staining was used for the nucleus, and antibodies against either -tubulin, a main component of the tubulin dimer that polymerises to form microtubules or against acetyl-α-tubulin, an indicator of stabilised microtubules, were used to visualise microtubule structure [16].

MBZ, ABZ and paclitaxel treatments all produced the condensed nuclei characteristic of apoptosis. α-tubulin and acetylated-α-tubulin both displayed a decreased fluorescent intensity following MBZ and ABZ treatment compared to control. By contrast, paclitaxel increased intensity of both α- and acetylated-α -tubulin staining compared to control. This suggests that MBZ and ABZ promote depolymerisation of microtubules, whereas paclitaxe l promotes polymerisation and stabilises microtubules, as expected.

MBZ and ABZ induce caspase-3 activity

Since it appeared that cell death was occurring concurrently with a block in the cell cycle, characteristics associated with various forms of apoptosis were investigated. Caspase-3 activity was measured in HT-29 cells following treatment with MBZ, ABZ, paclitaxel or vehicle-only control as before (Fig. 2a). Both untreated control and DMSO vehicle control showed low levels of activity. ABZ and MBZ treatment both increased caspase activation around 550-fold at 24 hours ($P < 0.0001$ compared to untreated control), which dropped back to 300-400 fold at 48 hours, suggesting that the cell death process had peaked within the first 24 hours. Paclitaxel treatment caused the greatest increase caspase activity, up to 750-fold of control at 24 hours ($P < 0.0001$ compared to MBZ, ABZ and controls), which is not surprising as paclitaxel is a classical apoptosis inducer and activates caspase-3 [17].

MBZ and ABZ cause early phosphatidylserine exposure

Following both 24 and 48 hr treatments, cells were double-stained with fluorescently labelled Annexin-V to identify early externalisation of phosphatidylserine residues, and PI to separate out the internal phosphatidylserine exposed to Annexin-V by cell membrane permeability, occurring as a result of primary or secondary necrosis (Fig. 2b,c). Following 24hr treatment, MBZ and ABZ caused approximate 25% decreases in the percentage of viable cells (negative for both Annexin V and PI) compared to control ($P < 0.0001$), similar to that of the positive control paclitaxel (Fig. 2b). MBZ and ABZ caused a significant increase in the percentage of cells with phosphatidylserine exposure, with 22.83% of MBZ treated cells and 24.17% of ABZ treated cells positive for Annexin V only, similar to paclitaxel at 20.72%, whereas only 3.37% of control cells were positive ($P < 0.0001$). Numbers of double stained cells undergoing secondary necrosis after treatment with paclitaxel, MBZ and ABZ all significantly increased to MBZ 5.78%, ABZ 5.99% and paclitaxel 7.94% vs control 2.12% ($P < 0.0001$). Necrotic cells, positive for PI only, were increased only in MBZ and ABZ treatments compared to control, 3.58% and 3.48% vs 0.54% respectively. Forty-eight-hour treatments produced similar results to that of 24hr treatments.

MBZ and ABZ treatment results in DNA fragmentation

Another indicator of apoptosis is the fragmentation of DNA content, known as sub-G1 DNA, measured using fixation of cells and PI staining. Here, following both 24 and 48hr treatments with MBZ, ABZ and paclitaxel, the percentage of cells with sub-G1 DNA content was significantly increased compared to control (Fig. 2d). After 24hrs, MBZ treatment resulted in 13.84% ($P = 0.001$) of cells with sub-G1 DNA content, ABZ 11.53% ($P = 0.026$), paclitaxel 19.33% ($P < 0.0001$) and control 6.45%. DMSO caused no statistically significant change. Following 48hr treatment, all amounts increased, except in the controls.

MBZ and ABZ increase mitochondrial membrane permeability

HT-29 cells were treated with MBZ, ABZ, paclitaxel, DMSO or left untreated for 24 and 48 hrs and the percentage of cells with higher mitochondrial membrane permeability, indicative of apoptosis, determined using the mitochondrial-targeted stain TMRE.

In the 24hr treatments, there were no significant differences between DMSO vehicle control (3.49 ± 0.38%) and control (3.36 ± 0.29%, $P > 0.05$). However, in MBZ, ABZ and paclitaxel treatments there were approximate 6-fold increases in the percentage of cells with permeabilised mitochondrial membranes (Fig. 2e). Cells exposed to the treatments for 48 hrs exhibited similar results, suggesting that the majority of cells had passed through the earlier phases of apoptosis by this time.

MBZ and ABZ induce oxidative stress, resulting reduced thiol oxidation

Indirect measurement of reactive oxygen species damage was undertaken using the DTNB assay, which quantifies reduced thiol content, from both protein and glutathione sources. This decreases as a consequence of oxidative stress. Following 48hr treatments, the reduced thiol concentration was significantly decreased in cells treated with MBZ, to 2.671×10^{-5} M ($P = 0.0094$), ABZ to 2.646×10^{-5} M ($P = 0.0086$) and paclitaxel to 2.539×10^{-5} M ($P = 0.0058$) in comparison to the control at 4.630×10^{-5} M (Fig. 2f).

Discussion

The colon cancer cells, HT29, were the most sensitive to MBZ and ABZ with IC_{50}s of 1.3 ± 0.1 μM and 1.4 ± 0.1μM for MBZ and ABZ respectively at 24 hours, and 0.11 ± 0.07 μM and 0.69 ± 0.42 μM at 48 hours. At 48 hours, the HT29 cells were 10- (MCF-7) or 136-fold (MDA-MB-231) more sensitive to MBZ and 12- (MCF-7) or 77-fold (MDA-MB-231) more sensitive to ABZ than the breast cancer types tested. While direct comparisons between cancer types have not been made before, similar levels of potency to HT29s have been found in gastric cancer cells for MBZ [6] and ABZ [11] and in squamous cell carcinoma cell lines [8], whereas cell lines representing other cancer types were much less sensitive [7,9,10].

MBZ and ABZ also show selectivity for cancer cells. Much higher concentrations were required to reduce the number of mesenchymal stromal cells. This is supported by previous results showing similar effects in fibroblasts (WI-38), endothelial cells (HUVEC) [3] keratinocytes [8], human foreskin fibroblasts [6] and primary canine fibroblasts [7].

In terms of the mechanism of action, we have shown that in HT29 cells, MBZ and ABZ both decrease proliferation and increase cell death levels. The drugs induce classical apoptosis, characterised by caspase-3 activation, mitochondrial membrane permeability and potential loss, phosphatidylserine exposure, DNA fragmentation and some oxidative stress. Nuclear morphology is also typical of apoptosis, including condensation and blebbing.

The activation of caspases by MBZ and ABZ has been shown before, in a range of cancer cell types, including squamous cell carcinoma [8], gastric cancer [6,11], melanoma [18], leukemia cells [19] and the HT29 cell line [20]. The generation of reactive oxygen species has been demonstrated once before, by ABZ in leukemia cells [19].

Other features of apoptosis have also been demonstrated previously, in separate studies. Phosphatidylserine exposure has been found with MBZ in melanoma [18] and ABZ in gastric cancer cells [11]. Mitochondrial involvement in cell death has been shown by cytochrome *c* release in lung cancer cells treated with MBZ [3,4]. ABZ alters the mitochondrial membrane potential of MCF-7 cells, but only at 100 μM [5].

In combination with apoptosis, we have shown that these anti-helmintics also induce a block in the cell cycle at G2/M in HT29 cells, as well as a related depolarisation of microtubules, which is likely to lead to mitotic arrest. The G2/M block is similar to what is found with paclitaxel and has also been shown using ABZ in gastric cancer lines [6,11] and MBZ in lung cancer cell lines [3,4].

Similar changes in microtubules to what was observed in HT29 cells treated with MBZ or ABZ have been found in other cancer cell types and described in a variety of ways. Depolymerisation of tubulin was found as a result of ABZ treatment in leukemia cells [19], ovarian cancer [10], canine glioma [7] and gastric cancer [11] and with MBZ in lung cancer cells [4]. In these last two studies, spindle formation was also shown to be inhibited. In melanoma cells, MBZ treatment caused diffuse staining with anti-alpha-tubulin antibody, showing microtubule disarray [18]. MBZ and ABZ treatment have also been shown to increase the ratio of soluble to insoluble tubulin in cancer cells, indicating tubulin depolymerisation. This was demonstrated for MBZ in lung cancer cells [4] and ABZ in gastric cancer cells [11].

The findings presented here systematically characterise the classical apoptotic cell death caused by anti-helmintic drugs MBZ and ABZ in cancer cells. The apoptotic death is connected to a G2/M cell cycle arrest and the depolymerisation of microtubules. These findings strengthen and bring together the already available but fractured evidence in a wide range of other cancer cells types. We further show that MBZ and ABZ are selective, being many-fold more potent in cancer cells compared to non-cancerous cell types, and also demonstrate that anti-helmintics do not show equal efficacy against every cancer cell type, but do appear to be effective against the colorectal cancer cell line HT29.

Declarations

Funding: This research was supported by the Department of Pharmacology and Toxicology, School of Biomedical Sciences, University of Otago.

Conflicts of interest/Competing interests: The authors have no conflicts of interest to declare.

Availability of data and material: All data are available from the corresponding author upon reasonable request.

Authors' contributions: SKB designed the study and experiments and prepared the manuscript, JSSMP carried out the experiments and the data analysis and contributed to the manuscript.

Code availability: Not applicable.

Ethics approvals: Not applicable.

Consent to participate: Not applicable.

Consent for publication: Not applicable.

Clinical trials information: Not applicable.

Acknowledgements: We acknowledge funding from the Department of Pharmacology and Toxicology, School of Biomedical Sciences, University of Otago.

References

1. Nygren P, Larsson R (2013) Drug repositioning from bench to bedside: tumor remission by the antihelmintic drug mebendazole in refractory metastatic colon cancer. Acta Oncol 53:427–428
2. Russell GJ, Lacey E (1995) Inhibition of [3H] mebendazole binding to tubulin by structurally diverse microtubule inhibitors which interact at the colchicine binding site. Biochem Mol Biol Int 35:1153–1159
3. Mukhopadhyay T, Sasaki J, Ramesh R, Roth JA (2002) Mebendazole elicits a potent antitumor effect on human cancer cell lines both in vitro and in vivo. Clin Cancer Res 8:2963–2969
4. Sasaki J, Ramesh R, Chada S, Gomyo Y, Roth JA, Mukhopadhyay T (2002) The antihelmintic drug mebendazole induces mitotic arrest and apoptosis by depolymeriseing tubulin in non-small cell lung cancer cells. Mol Cancer Ther 1(13):1201–1209
5. Castro LSEPW, Kviecinski MR, Ourique F, Parisotto EB, Grinevivius VMAS, Correia JFG, Filho DW, Pedrosa RC (2016) Albendazole as a promising molecule for tumor control. Redox Biol 10:90–99
6. Pinto LC, Mesquita FP, Soares BM, da Silva EL, Puty B, de Oliveira EHC, Burbano RR, Montenegro RC (2019) Mebendazole induces apoptosis via C-MYC inactivation in malignant ascites cell line (AGP01). Tox In Vitro 60:305–312
7. Lai SR, Castello SA, Robinson AC, Koehler JW (2017) In vitro anti-tubulin effects of mebendazole and fenbendazole on canine glioma cells. Vet Comp Oncol 15(4):1445–1454
8. Zhang QL, Lian DD, Zhu MJ, Li XM, Lee JK, Yoon TJ, Lee JH, Jiang RH, Kim CD (2019) Antitumor effect of albendazole on cutaneous squamous cell carcinoma (SCC) cells. BioMed Res Int, Volume 2019, Article ID 3689517, 9 pages
9. Liu H, Sun H, Zhang B, Liu S, Deng S, Weng Z, Zuo B, Yang J, He Y (2020) ^{18}F-FDG PET imaging for monitoring the early anti-tumor effect of albendazole on triple negative breast cancer. Breast Cancer 27:372–380, 2020
10. Chu SWL, Badar S, Morris DL, Pourgholami MH (2009) Potent inhibition of tubulin polymerisation and proliferation of paclitaxel-resistant 1A9PTX22 human ovarian cancer cells by albendazole. Anticancer Res 29:3791–3796, 2009

11. Zhang X, Zhao J, Gao Z, Pei D, Gao C (2017) Anthelmintic drug albendazole arrests human gastric cancer cells at the mitotic phase and induces apoptosis. Exp Ther Med 13:595–603
12. Williamson T, Bai RY, Staedtke V, Huso D, Riggins GJ (2016) Mebendazole and a non-steroidal anti-inflammatory combine to reduce tumor initiation in a colon cancer preclinical model. Oncotarget 7(42):68571–68584
13. Patel K, Doudican NZ, Schiff PB, Orlow SJ (2011) Albendazole sensitizes cancer cells to ionizing radiation. Rad Oncol 6:160
14. Mosmann T (1983) Rapid colorimetric assay for cellular growth and survival: application to proliferation and cytotoxicity assays. J Immunol Methods 65(1–2):55–63
15. Ellman GL (1959) Tissue sulfhydryl groups. Arch Biochem Biophys 82(1):70–77
16. Al-Bassam J, Corbett KD (2012) Alpha-tubulin acetylation from the inside out. Proc Natl Acad Sci U S A 109(48):19515–19516
17. Oyaizu H, Adachi Y, Taketani S, Tokunaga R, Fukuhara S, Ikehara S (1999) A crucial role of caspase 3 and caspase 8 in paclitaxel-induced apoptosis. Mol Cell Biol Res Commun 2(1):36–41
18. Doudican N, Rodriguez A, Osman I, Orlow SJ (2008) Mebendazole induces apoptosis via Bcl-2 inactivation in chemoresistant melanoma cells. Mol Cancer Res 6(8):1308–1315
19. Wang LJ, Lee YC, Huang CH, Shi YJ, Chen YJ, Pi SN, Chou YW, Chang LS (2019) Non-mitotic effect of albendazole triggers apoptosis of human leukemia cells via SIRT3/ROS/p38 MAPK/TTP axis-mediated TNFa upregulation. Biochem Pharmacol 162:154–168
20. Pourgholami MH, Akhter J, Wang L, Lu Y, Morris DL (2005) Antitumor activity of albendazole against the human colorectal cancer cell line HT-29: in vitro and in a xenograft model of peritoneal carcinomatosis. Cancer Chemother Pharmacol 55(5):425–432

Tables

Table 1

Cell line	**48 hours**	
	Mebendazole (MBZ)	Albendazole (ABZ)
MCF-7 Breast cancer cell line	1.1 ± 1.3 μM	8.1 ± 1.2 μM
MDA-MB-231 Breast cancer cell line	15.0 ± 0.1 μM	53.3 ± 0.2 μM
HT29 Colon cancer cell line	0.11 ± 0.07 μM	0.69 ± 0.42 μM
Mesenchymal stem cells	19.9 ± 0.1 μM	129.5 ± 0.1 μM

Figures

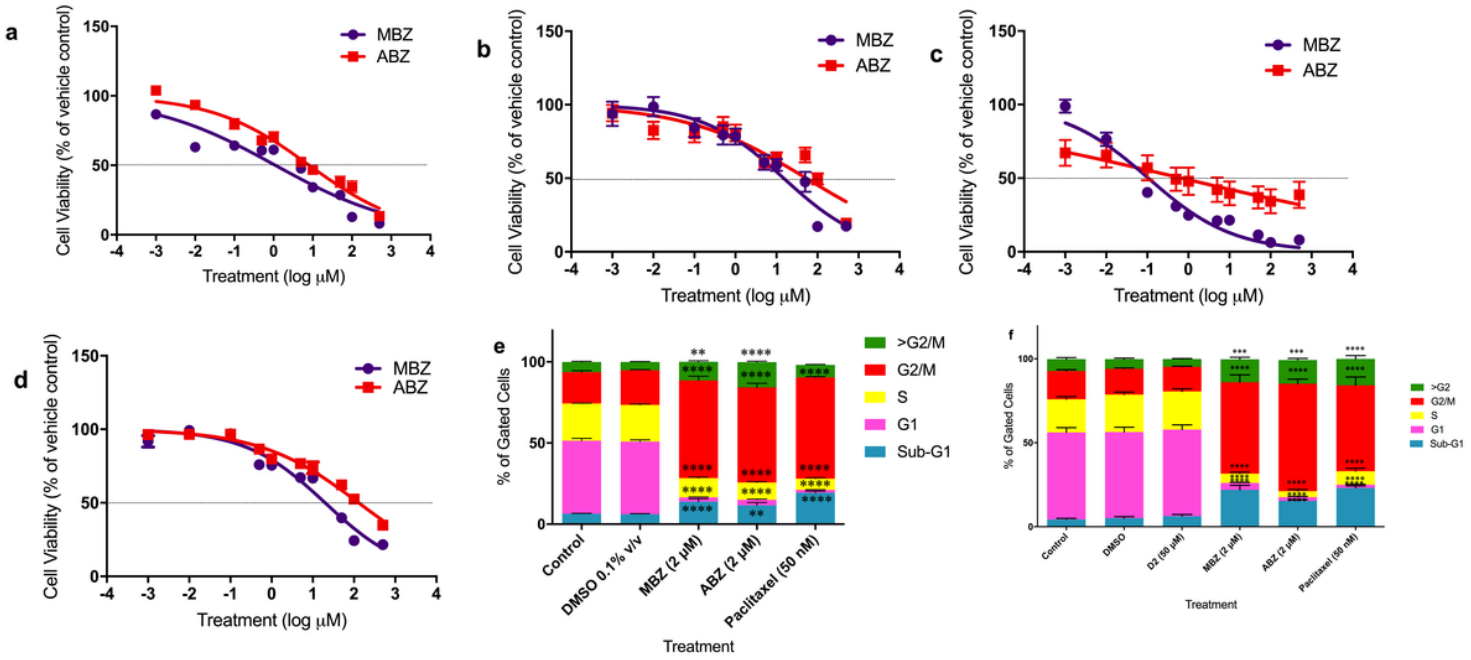

Figure 1

MBZ and ABZ reduce the cell number of cancer cell lines by inducing G2/M block and disrupting microtubule networks. Fig. 1 a-d: The MCF-7 (breast, Fig. 1a), MDA-MB-231 (breast Fig. 1b), HT-29 (colorectal, Fig. 1c) and RCB2157 (mesenchymal stem cell, Fig 1d) lines were treated with MBZ, ABZ (1 nM – 500 μM) or DMSO vehicle control (0.1% v/v) for 48 hrs, and relative cell number measured with MTT assays. IC50 values and line-of-best-fit calculated using non-linear regression. Each data point represents means ± SEM of three independent experiments (N=3) carried out in quadruplicate. Fig. 1e-f: Following a 24hr (Fig. 1e) or 48hr (Fig 1f) treatment of HT29 cells, DNA content was analysed using PI staining. Data represents mean ± SEM of the percentage of cells at each cell cycle stage (Sub-G1; G1; S; G2/M; >G2/M). Three independent experiments were conducted in triplicate with a minimum of 50,000 stopping events for each sample. Data was analysed using a two-way ANOVA with Dunnett's post-hoc test comparing to control, where $p < 0.05$ was considered statistically significant. **P < 0.01, ****P < 0.0001. Fig. 1g: HT-29 cells were treated with MBZ (2 μM), ABZ (2 μM), paclitaxel (50 nM) or DMSO vehicle control (0.1% v/v) for 8 hrs. Cells were stained with Hoechst 33342, anti-alpha-tubulin and anti-acetylated-alpha-tubulin and imaged using the Nikon AI-R inverted fluorescent microscope with Nikon Intensilight C-HGFI mercury lamp (Olympus, Japan) at 20x magnification, with consistent exposure.

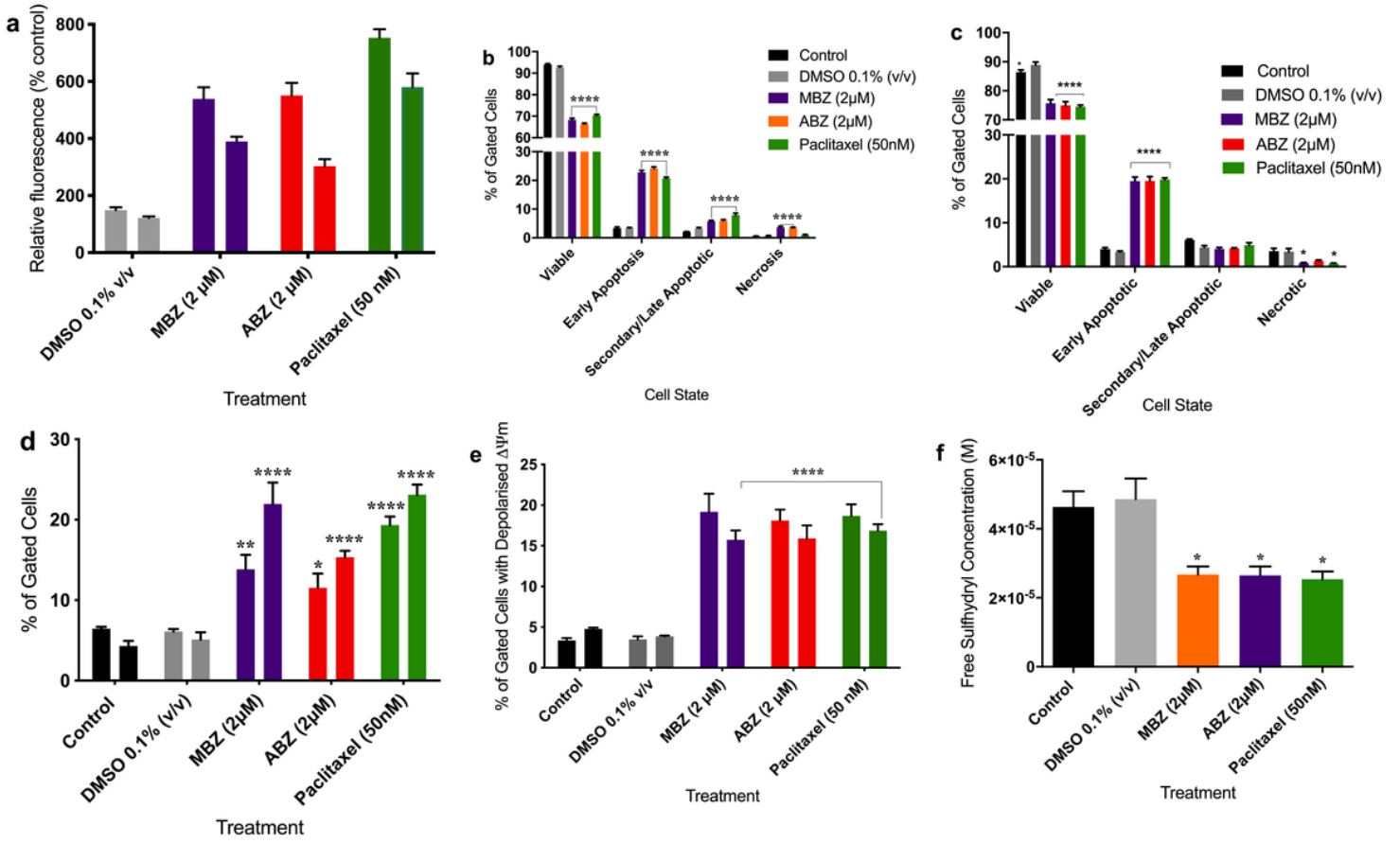

Figure 2

MBZ and ABZ induce classical apoptosis in HT29 colorectal cancer cells. HT29 cells were treated with MBZ, ABZ or DMSO vehicle control for 24 or 48 hrs, then stained for flow cytometry, fluorometry or spectroscopy. Fig. 2a: MBZ, ABZ and paclitaxel increase caspase-3 activity. Caspase-3 activity measured by fluorescent intensity using Ac-DEVD-AMC. Fig. 2b (24 hrs) and 2c (48 hrs): MBZ, ABZ and paclitaxel increase phosphatidylserine exposure. Percentage of HT-29 cells in viable (Annexin V-/PI-), early apoptotic (Annexin V+/PI-), secondary/late necrotic (Annexin V+/PI+), or necrotic (Annexin V-/PI+) states, determined by staining with Annexin V and PI. Fig. 2d: MBZ, ABZ and paclitaxel increase sub-G1 DNA content, following 24 hr (left bar) and 48 hr (right bar) treatment. Fig. 2e: MBZ, ABZ and paclitaxel cause depolarisation of the mitochondrial membrane potential (Ψ), determined by TMRE fluorescence intensity, following 24 hr (left bar) and 48 hr (right bar) treatment. Fig. 2f: MBZ, ABZ and paclitaxel decrease cellular free sulfhydryl content. The concentration of free sulfhydryls (M) in HT-29 cells was determined following 48 hr treatment. Data represents mean ± SEM of three independent experiments carried out in triplicate (N = 3). Data was analysed using a one-way ANOVA with Dunnett's post-hoc test comparing to control, where $P < 0.05$ was considered statistically significant. *$P < 0.05$, **$P < 0.01$, ****$P < 0.0001$